Ellipsometric and Raman spectroscopic study of nanocrystalline silicon thin films prepared by a rf magnetron sputtering technique

2008 J. Phys.: Condens. Matter 20 445221

(http://iopscience.iop.org/0953-8984/20/44/445221)

J. Phys.: Condens. Matter **20** (2008) 445221 (6pp) doi:10.1088/0953-8984/20/44/445221

Ellipsometric and Raman spectroscopic study of nanocrystalline silicon thin films prepared by a rf magnetron sputtering technique

Y Bouizem[1,3], C Abbes[1], J D Sib[1], D Benlakehal[1], R Baghdad[1], L Chahed[1], K Zellama[2] and S Charvet[2]

[1] Laboratoire de Physique des Couches Minces et Matériaux pour l'Electronique, Université d'Oran, Es-Sénia 31100, Algeria
[2] Laboratoire de Physique de la Matière Condensée, Faculté des Sciences, Université de Picardie Jules Verne, 33 rue Saint-Leu, 80039 Amiens, France

E-mail: ybouizem@hotmail.com

Received 17 May 2008, in final form 18 August 2008
Published 10 October 2008
Online at stacks.iop.org/JPhysCM/20/445221

Abstract

The structure of nanocrystalline silicon thin films (nc-Si:H) deposited by rf magnetron sputtering of a high-purity crystalline silicon target using argon (30%) and hydrogen (70%) gas mixture, under different pressures (P = 2, 3 and 4 Pa) and different substrate temperature (T_s = 100, 150 and 200 °C), has been studied with spectroscopic ellipsometry (SE; 1.5–5 eV) complemented with Raman spectroscopy measurements. The ellipsometry data were carefully analyzed using the Brüggeman effective medium approximation and the Tauc–Lorentz model. The results of this investigation clearly show that the samples deposited at 2 Pa present a completely amorphous structure whatever the substrate temperature, while those deposited at 3 and 4 Pa exhibit a nanocrystalline structure. These results suggest the existence of a threshold pressure around 3 Pa for which crystallization occurs. The samples are well crystallized with a crystalline volume fraction ranging from about 60 to 90%, and exhibit a mixture of small and large crystallite sizes. The deposition temperature has practically no effect on the size of the crystallites and on the average crystalline volume fractions. These results are in good agreement with the Raman spectroscopy data, and suggest the formation of Si crystallites in the gas phase. The analysis of the ellipsometric spectra also shows that the bulk layer is initiated from an amorphous interface (a-Si:H) present in the first steps of the growth, and is followed by a less crystallized subsurface layer.

1. Introduction

For more than a decade, hydrogenated nanocrystalline silicon (nc-Si:H) has received much interest and has been studied intensively from the points of view of both applications and fundamental physics. Due to its specific microstructure this material exhibits a lower density of localized states [1] and has various promising applications in solar cells and electronic domains [2–4]. Nanocrystalline silicon has a complex morphology consisting of a multilayered structure along the growth direction. This structure is heterogeneous and is, in principle, well defined. It consists of a hydrogenated amorphous silicon matrix (a-Si:H) in which ordered silicon clusters and/or crystallites with different size are embedded [5]. In addition, there are voids and disordered silicon tissues between the different phases. As a consequence, a very little is known about its localized states, and the understanding of its transport and phototransport properties is still at a rudimentary step.

It is well known that the performance of optoelectronic devices is greatly affected by the growth mechanism of

[3] Author to whom any correspondence should be addressed.

the material. The challenge is now to obtain improved materials at low temperature (well below typical processing temperature of 250–300 °C), and to understand the growth mechanism. From this point of view, deposition techniques including ion bombardment or not, such as in rf plasma enhanced chemical vapor deposition (PECVD) and hot wire CVD techniques, have been used to prepare a variety of microcrystalline silicon films (μc-Si:H) of high structural quality with different grain sizes and different hydrogen content and bonding configurations [6–8]. Besides of all these experimental works, a variety of growth models within the framework of surface and bulk reaction including a long range of hydrogen effects have been addressed [9–11]. However, very little is known about the microstructure and the growth processes of the rf-magnetron sputtered films.

As is well known, UV–visible spectroscopic ellipsometry (SE) is a powerful technique commonly used and well adapted to characterize this kind of material [12]. In order to give further experimental information about the correlations between the microstructure of the nc-Si:H films obtained by rf magnetron sputtering technique and the deposition parameters, the films are investigated using SE experiments complemented by Raman spectroscopy ones.

2. Experimental procedure and method of analysis

Three series of samples were deposited on fused silica by rf sputtering of high-purity crystalline silicon target using an argon (30%) and hydrogen (70%) gas mixture under different pressures: $P = 2$, 3 and 4 Pa. For each pressure, three different values of substrate temperature T_s (100, 150 and 200 °C) were used. The substrates were ultrasonically cleaned in successive baths of trichlorethylene, acetone and propanol before loading into the chamber. All the samples were prepared at a rf power density of 0.9 W cm^{-2}. These conditions lead to typical deposition rates of 0.7–4 Å s^{-1}. The microstructure of the obtained films is then studied by spectroscopic UV–visible (1.5–5 eV) phase modulated ellipsometry (Jobin Yvon). The data are analyzed using the Brüggeman effective medium approximation (BEMA) [13] and the Tauc–Lorenz model [14]. They are complemented by Raman spectroscopy using an Ar^+ laser beam (514.5 nm) with a low incident power of 2 mW, in order to avoid any beam induced crystallization during analysis, and carried out in the 100–600 cm^{-1} frequency range, and also used to estimate the crystalline volume fractions from the transverse optical (TO) phonon mode (520 cm^{-1}).

In any ellipsometry experiment, one measures the changes in the state of the polarization of a monochromatic beam upon reflection at an optical boundary. The changes are expressed in terms of two angles, ψ and Δ, by the following equation:

$$\tilde{\rho} = \frac{\tilde{r}_p}{\tilde{r}_s} = \mathrm{tg}\,\psi\, \mathrm{e}^{\mathrm{i}\Delta} \tag{1}$$

where $\tilde{r}_p$ and $\tilde{r}_s$ are the complex amplitude reflection coefficients for a plane wave polarized parallel and perpendicular to the plane of incidence, respectively. The ellipsometric parameters Δ and tgψ characterize, respectively, the phase difference between the two polarizations and the amplitude ratio.

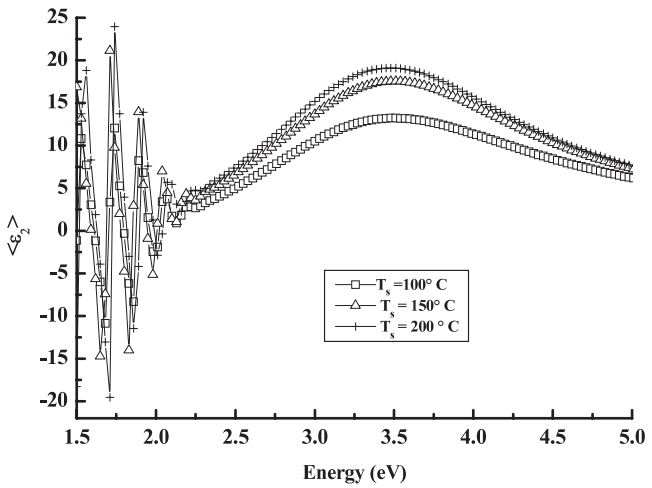

Figure 1. Effect of the deposition temperature on the imaginary part ε_2 of the pseudo-dielectric function of the samples deposited at 2 Pa and at three different T_s values, 100, 150 and 200 °C, as indicated.

In the particular case of an abrupt interface between two semi-infinite media the ellipsometric data are related to the complex dielectric function $\tilde{\varepsilon}$ by the following relation:

$$\tilde{\varepsilon} = \varepsilon_1 + \mathrm{i}\varepsilon_2 = n_0^2 \sin^2\phi \left\{1 + \left[(1-\tilde{\rho})/(1+\tilde{\rho})\right]^2 \tan^2\phi\right\} \tag{2}$$

where n_0 is the index of refraction of the medium where the waves propagate and ϕ is the angle of incidence.

In real cases, and because of the non-linearity of the relations, we used a multilayer optical model to fit SE data to obtain quantitative information. The model considers the number of layers covering the substrate as well as their thicknesses and their dielectric functions, resulting in improved fits. The regression analysis method consists in minimizing χ^2 as the figure of merit of the fitted function by varying the model parameters:

$$\chi^2(\theta) = \frac{1}{2N}\sum_{k=1}^{N} \frac{\left|I_{\mathrm{s\,cal}}(\theta,\lambda_k) - I_{\mathrm{s\,mes}}(\lambda_k)\right|^2}{\delta_k^2} + \frac{\left|I_{\mathrm{c\,cal}}(\theta,\lambda_k) - I_{\mathrm{c\,mes}}(\lambda_k)\right|^2}{\delta_k^2}. \tag{3}$$

Here, I_s and I_c are the measured currents at the wavelength λ, related to the ellipsometry parameters and well defined in the phase modulated ellipsometry technique [15, 16]. The subscripts 'mes' and 'cal' designate, respectively, the measured values and those calculated within the theoretical model. The number of unknown model parameters is denoted by θ, while N is the number of measured data points, and δ_k is the weight introduced to take into account the statistical errors on $I_{\mathrm{s\,mes}}$ and $I_{\mathrm{c\,mes}}$.

3. Results and discussion

The imaginary part $\langle\varepsilon_2\rangle$ of the pseudo-dielectric functions deduced from the ellipsometry measurements for the series deposited under 2 Pa at different substrate temperatures is shown in figure 1. The shapes of the spectra are quite similar.

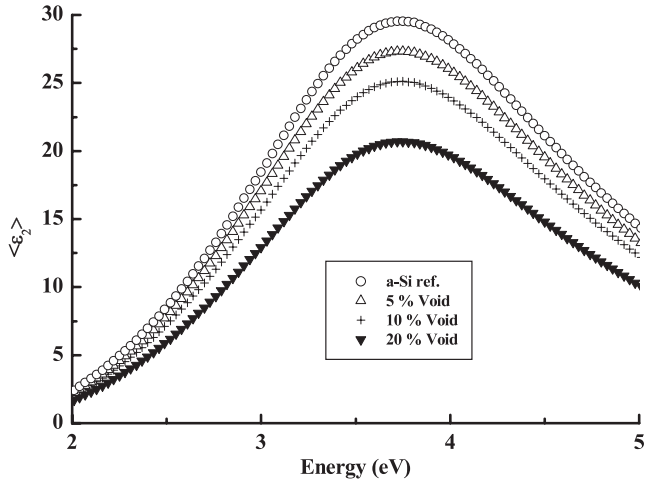

Figure 2. Effect of the void fraction on the imaginary part ε_2 of the pseudo-dielectric function of amorphous silicon calculated with BMEA, using a-Si structure and void constituents [17]. The dielectric function for a-Si reference is the one reported by Aspness [17].

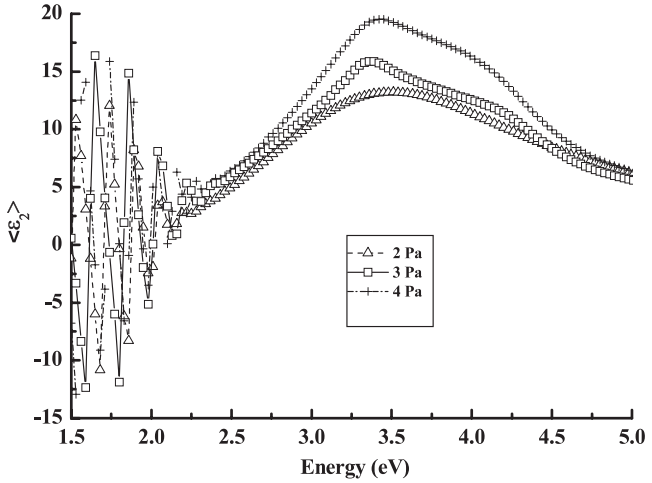

Figure 3. Example of the effect of the pressure on the imaginary part ε_2 of the pseudo-dielectric function of the samples deposited at 100 °C, and at different pressure values of 2, 3 and 4 Pa, as indicated.

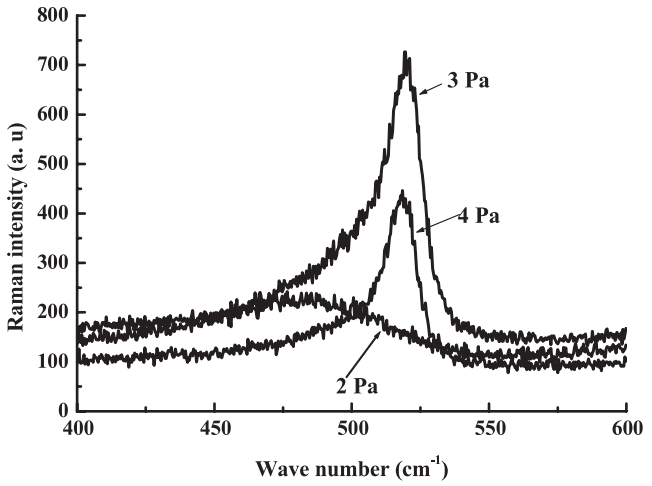

Figure 4. Example of typical Raman spectra of the samples corresponding to figure 3, deposited at 100 °C, and at different pressure values of 2, 3 and 4 Pa, as indicated.

In the low energy part of the spectra, $\langle\varepsilon_2\rangle$ exhibit interference fringes related to the large penetration depth of the light in the films. In the non-interference range, the spectra consist only of large peaks centered around 3.5 eV. The decrease of T_s from 200 to 100 °C leads to a decrease of the amplitude of $\langle\varepsilon_2\rangle$ without any significant shift of the maxima. The localization of the peak around 3.5 eV is often attributed to an amorphous structure, while the decrease of the $\langle\varepsilon_2\rangle$ intensity is related to a small density loss in the material. A clear and additional proof of these structural changes in the bulk of the material is gained from the numerical simulation shown in figure 2. In this simulation, $\langle\varepsilon_2\rangle$ is calculated by using BEMA [13], taking into account the presence of only two constituents, amorphous silicon a-Si and void [17]. This approach gives a unique solution to define the film structure as expressed in terms of its constituents. In figure 2, which presents examples of different $\langle\varepsilon_2\rangle$ spectra calculated for different values of the void fraction, it is clearly seen that the increase in the void fraction leads to a decrease in the $\langle\varepsilon_2\rangle$ amplitude without any shift in the peak position. Therefore, we can conclude that the samples deposited under 2 Pa, that are associated with $\langle\varepsilon_2\rangle$ spectra (see figure 1) having similar shapes to those of figure 2, present a completely amorphous structure whatever the substrate temperature. The only effect of T_s is to decrease the voids fraction in the films, and consequently to increase the film compactness.

Figure 3 shows an example of the effect of the pressure on $\langle\varepsilon_2\rangle$ for the samples deposited at T_s of 100 °C. It can clearly be seen that the shapes of the spectra are quite different when the pressure varies from 2 to 3 and 4 Pa. For the 3 and 4 Pa samples, two peaks are observable. One main peak around 3.4 eV and one less intense shoulder around 4.2 eV. They correspond to a convolution of direct electronic transitions in the UV region of the crystalline silicon. These features are an obvious signature of the presence of a crystalline Si structure in the films. We obtain the same type of spectral shapes the series deposited at 150 and 200 °C and under their corresponding different pressures. These results clearly show a transition from a completely amorphous phase to another one with crystalline Si when the pressure is raised from 2 to 3 and 4 Pa. They also suggest the existence of a threshold pressure around 3 Pa for which crystallization occurs, independently of the substrate temperature.

The ellipsometric results are in good agreement with those obtained by Raman spectroscopy experiments. Indeed, figure 4 shows typical Raman spectra obtained in the transverse optic (TO)-like mode corresponding to the samples of figure 3. As expected, the spectrum of the film deposited at 2 Pa presents only a broad peak centered at 480 cm^{-1}, confirming the completely amorphous structure of this film [18, 19]. On the contrary, the spectra corresponding to the samples deposited under 3 and 4 Pa exhibit a narrow and predominant peak located around 520 cm^{-1} which suggests the presence of the crystalline Si in the films, in addition to a much smaller shoulder at 480 cm^{-1}. We obtain the same type of

Table 1. Results of the analysis of the Raman and the ellipsometric spectroscopic spectra, obtained for the samples deposited at 3 and 4 Pa, for three T_s (100, 150 and 250 °C). The dispersion of the error bars is estimated negligible. Only the maximum value of the error obtained is indicated for each parameter.

	f_c (%) ellipsometric results		f_c (%) Raman results	
T_s (°C)	3 Pa	4 Pa	3 Pa	4 Pa
100	85 ± 5	60 ± 5	75 ± 5	90 ± 5
150	87 ± 5	59 ± 5	79 ± 5	89 ± 5
200	86 ± 5	62 ± 5	85 ± 5	85 ± 5

spectral features for the 150 and 200 °C deposited samples, under the corresponding different pressures. Both Raman and ellipsometry spectra give crystalline signatures. Similar results have been obtained on PECVD silicon nano-crystalline films [20]. From the integrated intensity of the peak corresponding to the amorphous phase I_a (480 cm^{-1}) and of that associated with the crystalline one I_{cr} (520 cm^{-1}), and using the procedures presented in previous works [19, 21], we can estimate the crystalline volume fraction defined by the ratio:

$$f_c = \frac{I_{cr}}{I_a + I_{cr}}. \tag{4}$$

The results obtained for f_c are summarized in table 1.

Let us now return to the analysis of the SE data. According to the growth mechanisms discussed in the literature [22, 23], the interpretation of SE data requires optical models with several layers, where the dielectric function of each layer and its thickness must be known. Usually, the heterogeneous character of a microcrystalline silicon layer is described by a pseudo-dielectric function modeled by using the BEMA [13] consisting of an amorphous silicon matrix in which Si crystallites with different sizes and voids are incorporated. However, in the modeling of the effective dielectric function, the a-Si structure proposed by Aspness [17], which is a dense material, is often used and the effect of hydrogen is generally omitted. This method results in approximate fits to the experimental data. To avoid this problem and to improve the quality of the fits our methodology consists in the first attempt to determine the correct dielectric function of the amorphous phase reference. Thus, our a-Si:H reference is assumed to be the one deposited under 2 Pa and at different T_s. The analysis of the corresponding spectra was performed using a two-layer model: substrate/bulk/surface roughness. To derive the complex dielectric function of the bulk material, we used the Tauc–Lorentz model [14], which is particularly well suited to fit the dielectric function of an amorphous semiconductor above the band edge. In this model, the energy dependence of ε_2 is modeled as the product of the Tauc joint density of states [14] with a Lorentz oscillator:

$$\varepsilon_2(E) = \begin{cases} \dfrac{AE_0C(E-E_g)^2}{(E^2-E_0^2)^2 + C^2E^2}\dfrac{1}{E} & \text{for } E \geqslant E_g \\ 0 & \text{for } E \leqslant E_g \end{cases} \tag{5}$$

where A is the amplitude factor, which is proportional to the density of the material and to the optical transition matrix elements, C is the broadening parameter that is universally related to the short range order, E_0 is the peak transition and E_g is the optical band gap.

The real part of the dielectric function ε_1 is obtained by Kramers–Kronig integration of ε_2:

$$\varepsilon_1(E) = \varepsilon_1(\infty) + \frac{2}{\pi} P \int_{E_g}^{\infty} \frac{E'\varepsilon_2(E)}{E'^2 - E^2}\, dE'. \tag{6}$$

The integration introduces another parameter $\varepsilon_1(\infty)$. The surface roughness layer was modeled as formed by a mixture of bulk material (50%) and voids (50%), using the BEMA [13]. The fitting parameters are the Tauc–Lorentz dispersion law coefficients [14] and the thicknesses d and d_r, of the bulk and of the surface roughness layers, respectively. The optical response of the system is calculated by the generalization of the Fresnel laws [24] and fitted to the SE data. The minimization of χ^2 function was performed in the whole spectral range (1.5–5 eV). The interference fringes were taken into account to obtain a more accurate thicknesses of the films and to avoid strong correlation of the fitting parameters. Following this methodology, quite correct fits to the data were obtained ($\chi^2 < 1$), and none of the cross-correlation coefficients exceeds 0.38. The results of this analysis are summarized in table 2, for the films deposited at 2 Pa. As expected, these results fit a general tendency, as already reported in the literature [25, 26]. As the substrate temperature T_s increases, the density of the material increases, while the optical gap E_g and the degree of disorder of the material decreases, respectively. The substrate temperature has practically no effect on the roughness surface layer.

In order to obtain quantitative information about the effect of the pressure on the microstructure of the films, and to have a schematic view of their growth mechanism, we have analyzed carefully the SE data obtained for the samples deposited at 3 and 4 Pa. In this analysis, we have tried various but reasonable optical models until the selected model yielded a good enough fit to the all the spectra. The methodology followed is first to pre-choose the simplest model consisting, as discussed above for the films deposited at 2 Pa, of two layers (a bulk layer covered by a roughness surface layer) and try to fit it to the experimental spectra. The two-layer fit has failed; we found, by numerical calculation with a random variation of all possible fitting parameters, that it was not possible to improve the fit to all the spectra (e.g. χ^2 is considerably greater than 1 for all the samples). Then, we move to the next step, by adding another layer, or by changing one of the constituents. The best model that well fitted our experimental SE data consisted of four layers, in good agreement with the growth mechanism processes proposed previously for PECVD polymorphous (pm-Si:H) and microcrystalline (μc-Si:H) silicon materials [22]. This model is as follows:

(i) The first layer is the interface layer with the substrate. It is completely amorphous (a-Si:H) and probably corresponds to an incubation phase during the first steps of the film growth mechanism.
(ii) The second layer is the bulk layer. It was modeled using the BEMA [13], consisting of a mixture of a-Si:H and Si

Table 2. Values of the thicknesses d and d_r of the bulk and of the roughness surface layers, respectively, and of the Tauc–Lorentz law parameters resulting from the fitting of the ellipsometric spectra for the samples deposited at 2 Pa and at different T_s. The dispersion of the error bars is estimated negligible. Only the maximum value of the error obtained is indicated for each particular parameter.

T_s (°C)	d (Å)	d_r (Å)	A	E_0 (eV)	E_g (eV)	C (eV)	ε_1 (∞)
100	8313 ± 24	29 ± 2	135 ± 2	3.56 ± 0.01	1.74 ± 0.01	2.34 ± 0.01	0.21 ± 0.01
150	7350 ± 24	27 ± 2	150 ± 2	3.62 ± 0.01	1.71 ± 0.01	2.11 ± 0.01	0.20 ± 0.01
200	6798 ± 24	30 ± 2	178 ± 2	3.59 ± 0.01	1.69 ± 0.01	2.08 ± 0.01	0.21 ± 0.01

crystallites of different sizes. Small and large grain sizes of polycrystalline silicon given by Jellisson *et al* [27] were used for the 3 Pa and 4 Pa samples, respectively.

(iii) The third layer is the subsurface layer which is in front of the plasma during the film growth. It was modeled as the bulk, with a lower thickness and a less crystallized phase.

(iv) The fourth layer is the roughness layer. It is considered as an overlayer formed by a mixture of layer 3 (50%) and voids (50%) and modeled using the BEMA [13].

The dielectric function of a-Si:H used in the present modeling is given for each temperature by the Tauc–Lorentz dispersion law with the parameters summarized in table 2. In this approach, there are only eight free parameters: the thicknesses of the different layers, and the volume fractions of the constituents of the bulk and subsurface layers. We have also tried a second approach by incorporating more degrees of freedom into the fitting procedure using the parameterization of the dielectric function of a-Si:H from the Tauc–Lorentz model [14]. But this second approach has failed, as on the one hand it needs five new free parameters and, on the other hand, the resulting values obtained for χ^2 from the different fits are considerably greater than those obtained using the first approach, for all the samples. The uniqueness of the solution is not guaranteed, since several combinations of parameters could equivalently fit the spectra.

We present in figures 5(a) and (b) an example of the experimental and fitted SE data obtained, respectively, for ε_1 and ε_2 for the sample deposited at 3 Pa and 100 °C. As mentioned above, the film morphology reveals a completely amorphous interface layer with the substrate ($d = (111 \pm 15)$ Å), a highly crystallized bulk ($f_c = (88 \pm 5)\%$, $d = (8219 \pm 20)$ Å), a less crystallized subsurface layer ($f_c = (68 \pm 5)\%$, $d = (412 \pm 20)$ Å) and a roughness surface layer ($d_r = (43 \pm 5)$ Å). A similar behavior is obtained for all the samples deposited at 3 and 4 Pa. The volume fractions of the constituents, averaged by their respective total thickness, are summarized in table 1. These results are in quite good agreement with those obtained by Raman spectroscopy measurements and reported in the same table for comparison. However, the f_c values estimated from the Raman results for the 4 Pa sample are slightly higher than those determined from the modeled SE data.

Two important points can be drawn from these results:

(i) The 3 and 4 Pa samples are crystallized with a mixture of crystallites with small and large grain sizes [27], with a larger proportion of small size grains in the 3 Pa films.

(ii) The crystalline volume fraction seems to be independent of the substrate temperature.

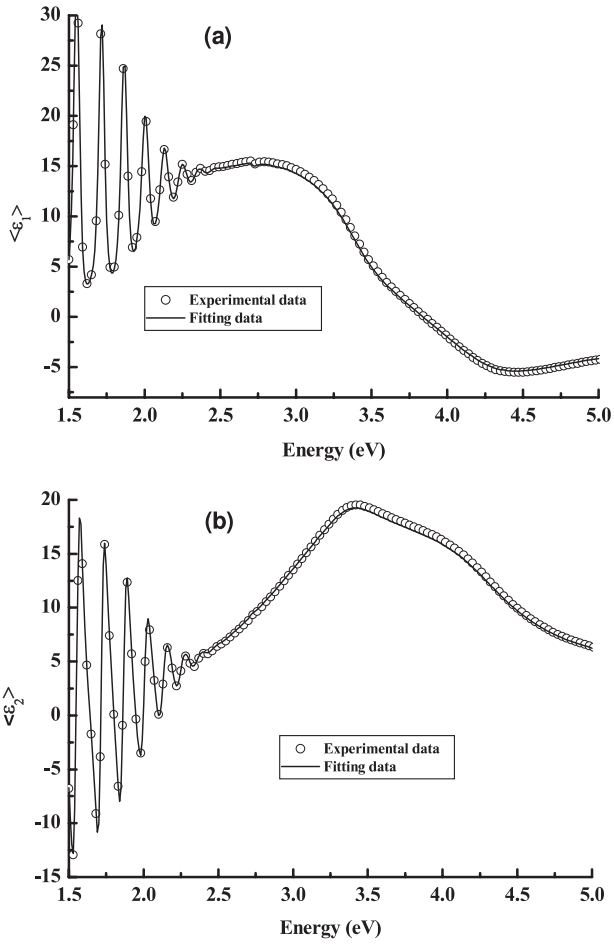

Figure 5. Example of experimental and fitted data of the real ε_1 and the imaginary ε_2 parts of the pseudo-dielectric function, respectively, obtained for the sample deposited at 3 Pa and 100 °C. The open symbols correspond to the data and the lines correspond to the fit.

From these results it appears that only the pressure plays a predominant role in the formation of the crystallites size and the crystalline volume fractions. The deposition temperature has practically no effect on the crystallization process, but seems to influence the compactness of the film, essentially in the completely amorphous 2 Pa deposited samples. Therefore, it can be suggested that the Si nanocrystallites are first produced in the gas phase and then they are incorporated in the a-Si:H matrix during film growth. A similar behavior has been previously reported for the rf PECVD μc-Si:H material [28].

4. Conclusion

The present study brings new results for the effects of pressure and the deposition temperature on the structural properties

of nc-Si:H films deposited by rf magnetron sputtering. The pseudo-dielectric function of these films, measured with spectroscopic ellipsometry, has been modeled using BEMA and the Tauc–Lorentz model and fitted carefully to the experimental data. The analysis suggests that the structure of the 2 Pa samples is completely amorphous. A pressure of about 3 Pa is optimum to obtain well crystallized films with a large proportion of small size grains. It seems that the deposition temperature does not affect the grain size and crystalline volume fraction considerably. These parameters depend only on the pressure. Finally, the production of crystalline silicon particles in the gas phase is suggested as a means of producing nc-Si:H by rf magnetron sputtering.

Acknowledgments

The authors would like to thank Dr M El Marssi for assistance with the Raman experiments. This work is kindly supported by the Accord-Program CMEP 04 MDU 614 and the French embassy in Algeria.

References

[1] Jia H, Saha J K, Ohse N and Shirai H 2006 *J. Non-Cryst. Solids* **352** 896
[2] Martins R, Macarico A, Ferreira I, Nunes R, Bicho A and Fortinato E 1997 *Thin Solid Films* **303** 47
[3] Klein S, Finger F, Carius R and Stutzman M 2005 *J. Appl. Phys.* **98** 24905
[4] Shah A V, Meier J, Vallat-Sauvan E, Wyrch N, Kroll U, Droz C and Grof U 2003 *Sol. Energy Mater. Sol. Cells* **78** 469
[5] Roca I Cabarrocas P, Hamma S, Sharma S N, Costa J and Bertran E 1998 *J. Non-Cryst. Solids* **871** 227
[6] Chakraborty K and Das D 2006 *Sol. Energy Mater. Sol. Cells* **90** 849
[7] Kondo M 2003 *Sol. Energy Mater. Sol. Cells* **78** 543
[8] Djeridane Y, Abramov Y and Roca i Cabarrocas P 2007 *Thin Solid Films* **515** 7451
[9] Das D 2003 *J. Phys. D: Appl. Phys.* **36** 2335
[10] Umemoto H, Ohara K, Morita D, Nozari Y, Matsuda A and Matsumura H 2002 *J. Appl. Phys.* **91** 1650
[11] Arthur N L and Miles L A 1998 *Chem. Phys. Lett.* **282** 192
[12] Azzam R M A and Bashara M N 1977 *Ellipsometry and Polarized Light* (Amesterdam: North-Holland)
[13] Bruggeman D A G 1935 *Ann. Phys., Lpz.* **24** 636
[14] Jellison G E Jr and Modine F A 1996 *Appl. Phys. Lett.* **69** 371
[15] Bermudez V M and Ritz V H 1978 *Appl. Opt.* **17** 542
[16] Drevillon B, Perrin J, Marbot R, Violet A and Dalby J L 1982 *Rev. Sci. Instrum.* **53** 969
[17] Aspness D E and Theeten J B 1980 *J. Electrochem. Soc.* **127** 1359
[18] Touir H, Dixmier J, Zellama K, Morhange J F, Bounouh Y and Elkaim P 1998 *J. Non-Cryst. Solids* **227** 906
[19] Goncalves C, Charvet S, Zeinert A, Clin M and Zellama K 2002 *Thin Solid Films* **403** 91
[20] Chaâbane N, Khachenko A V, Vach H and Roca i Cabarrocas P 2003 *New J. Phys.* **5** 37
[21] Baghdad R, Benlakehal D, Portier X, Zellama K, Charvet S, Sib J D, Clin M and Chahed L 2008 *Thin Solid Films* **516** 3965
[22] Kalache B, Kozarev A I, Vanderhaghen R and Roca i Cabarrocas P 2003 *J. Appl. Phys.* **93** 1262
[23] Amans D, Callard S, Gagnaire A and Joseph J 2003 *J. Appl. Phys.* **93** 4173
[24] Abéles F 1967 *Advanced Optical Techniques* ed A C S Van Heel (Amesterdam: North-Holland)
[25] Fontcuberta i Morral A and Rocca i Cabarrocas P 2004 *Phys. Rev.* B **69** 125307
[26] Daineka D, Suendo V and Roca i Cabarrocas P 2004 *Thin Solid Films* **468** 298
[27] Jellisson G E Jr, Chisholm M F and Gorbatkin S M 1993 *Appl. Phys. Lett.* **62** 3348
[28] Roca i Cabarrocas P 2000 *J. Non-Cryst. Solids* **266** 31